Available online at www.sciencedirect.com
SCIENCE DIRECT®
Journal of the Franklin Institute 342 (2005) 175–192
Journal of The Franklin Institute
www.elsevier.com/locate/jfranklin

Limit cycle analysis of nonlinear sampled-data systems by gain–phase margin approach

Bing-Fei Wu*, Jau-Woei Perng, Hung-I Chin

Department of Electrical and Control Engineering, National Chiao Tung University, 1001, Ta Hsueh Road, 300, Hsinchu, Taiwan, ROC

Abstract

This work analyzes the limit cycle phenomena of nonlinear sampled-data systems by applying the methods of gain–phase margin testing, the *M*-locus and the parameter plane. First, a sampled-data control system with nonlinear elements is linearized by the classical method of describing functions. The stability of the equivalent linearized system is then analyzed using the stability equations and the parameter plane method, with adjustable parameters. After the gain–phase margin tester has been added to the forward open-loop system, exactly how the gain–phase margin and the characteristics of the limit cycle are related can be elicited by determining the intersections of the *M*-locus and the constant gain and phase boundaries. A concise method is presented to solve this problem. The minimum gain–phase margin of the nonlinear sampled-data system at which a limit cycle can occur is investigated. This work indicates that the procedure can be easily extended to analyze the limit cycles of a sampled-data system from a continuous-data system cases considered in the literature. Finally, a sampled-data system with multiple nonlinearities is illustrated to verify the validity of the procedure.

Keywords: Limit cycle; Gain–phase margin; Sampled-data; Describing function

*Corresponding author.
E-mail address: bwu@cc.nctu.edu.tw (B.-F. Wu).

0016-0032/$30.00
doi:10.1016/j.jfranklin.2004.10.004

1. Introduction

Accurately predicting the limit cycles of nonlinear control systems has been relevant to many industrial applications using describing function method. Hydraulic and robotic control systems with friction have been addressed in recent years [1,2]. In [3], a car steering control with an actuator rate limit was considered. In addition, Amato et al. analyzed pilot-in-the-loop oscillations due to positional and rate saturations [4].

Although the controller of a linearized model can be designed by any classical or modern method, the limit cycle characteristics of the designed system must be thoroughly analyzed, since the system is likely to exhibit undesirable limit cycles caused by nonlinearities. Uncertain parameters in a linear control system can be robustly analyzed by the parameter plane method or the parameter space method [5–8]. The *M*-locus method can also be implemented to represent the describing function of nonlinearities in the parameter plane or parameter space to determine the characteristics of limit cycles [9]. The above methods can be used to decide carefully the safe range of system parameters to avoid the generation of limit cycles.

In the frequency-domain approach, gain margin (GM) and phase margin (PM) are two important indices for analyzing and designing practical control systems. Methods of analyzing the gain–phase margin in a linear continuous-data system with adjustable parameters have recently been developed [10]. This approach has been extended to analyze a nuclear reactor system with various transport lags [11] and a proportional navigation sampled-data control system [12]. Thereafter, the prediction of limit cycles in some nonlinear control systems, such as a reactor system and a low-flying vehicle, was analyzed in [13–15]. The authors of the current investigation also addressed the gain–phase margin analysis of pilot-induced oscillations for predicting limit cycles [16].

A systematic strategy, similar to [16], is first presented to predict the limit cycles caused by the effects of parameter variations and hard nonlinearities and, in doing so, to extend the above results to the sampled-data control systems. A simple method for evaluating the gain–phase margins and the *M*-locus in the parameter plane is also proposed for analyzing stability by inserting a gain–phase margin tester into the forward open-loop of a linearized sampled-data control system. Importantly, the developed approach is very easy to implement and can provide more information on limit cycles. Finally, two examples of nonlinear sampled-data system are given to confirm the proposed design procedures.

The rest of this paper is organized as follows. Section 2 presents the basic approach. Section 3 presents the first example of an aircraft pitch control system, including one nonlinear element provided to demonstrate the design procedures. Section 4 extends the approach to analyze a sampled-data control system with multiple nonlinearities. Finally, Section 5 draws conclusions.

2. Conventional approach

This section addresses the conventional approach in predicting the limit cycles of nonlinear sampled-data control systems.

2.1. Parameter plane analysis

A sampled-data control system with m nonlinearities $(n_1, n_2, \ldots, n_m)$ can generally be linearized by applying the classical describing function method. The equivalent linearized system with a gain–phase margin tester $(Ke^{-j\theta})$ added to the forward open-loop system is shown in Fig. 1. $G(z, N_{1R}, N_{1I}, \ldots, N_{mR}, N_{mI})$ is the open-loop transfer function, where the terms $N_{1R}, \ldots, N_{mR}$ and $N_{1I}, \ldots, N_{mI}$ are the real and imaginary parts of the describing function (N_i) of $n_1, n_2, \ldots, n_m$, respectively. The describing functions can be represented as follows:

$$N_i(A, \omega) = N_{iR}(A, \omega) + jN_{iI}(A, \omega), \quad i = 1, \ldots, m, \tag{1}$$

where A and ω represent the amplitude and frequency of a sinusoidal input to one of the nonlinearities. The characteristic equation of the linearized sampled-data control system can be expressed as

$$\begin{aligned} &1 + Ke^{-j\theta}G(z, N_{1R}, N_{1I}, \ldots, N_{mR}, \ldots, N_{mI}) \\ &\quad = 1 + Ke^{-j\theta}\,\frac{N(z, N_{1R}, N_{1I}, \ldots, N_{mR}, \ldots, N_{mI})}{D(z, N_{1R}, N_{1I}, \ldots, N_{mR}, \ldots, N_{mI})}, \\ &\quad = 0 \end{aligned} \tag{2}$$

which is equivalent to

$$\begin{aligned} f(z) \triangleq\!\!\triangleq\; &D(z, N_{1R}, N_{1I}, \ldots, N_{mR}, \ldots, N_{mI}) \\ &+ Ke^{-j\theta}N(z, N_{1R}, N_{1I}, \ldots, N_{mR}, \ldots, N_{mI}) = 0. \end{aligned} \tag{3}$$

Let $z = e^{j\omega T}$, where T is the sampling period; Eq. (3) is expressed as

$$f(e^{j\omega T}) = f(\alpha, \beta, \gamma, \ldots, K, \theta, j\omega T) = 0, \tag{4}$$

where $\alpha, \beta, \gamma, \ldots$ are variables determined by the terms (N_{iR}, N_{iI}) in the describing functions and/or the adjustable parameters of the linear part of the system [9]. Clearly, the designer can arbitrarily define these variables to analyze the effect of the system parameters. If only two parameters α and β are considered, then Eq. (4) can be classified as follows:

$$f(\alpha, \beta, \gamma, \ldots, K, \theta, j\omega T) = X\alpha + Y\beta + Z = 0, \tag{5}$$

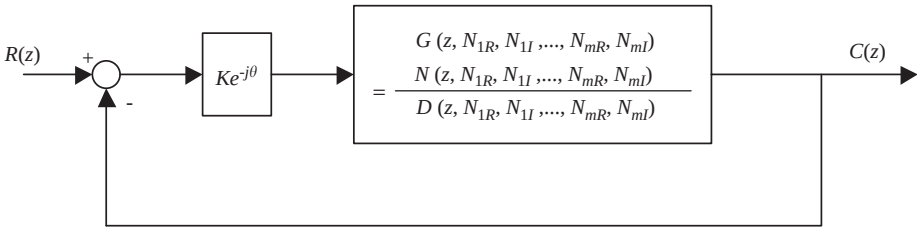

Fig. 1. Block diagram of a linearized sampled-data control system with a gain–phase margin tester.

where X, Y and Z are functions of $\gamma,\ldots,K,\theta$ and $j\omega T$. Dividing Eq. (5) into two stability equations with a real part (f_R) and an imaginary part (f_I), yields

$$f_R(\alpha,\beta,\gamma,\ldots,K,\theta,\omega T) = X_1\alpha + Y_1\beta + Z_1 = 0 \tag{6}$$

and

$$f_I(\alpha,\beta,\gamma,\ldots,K,\theta,\omega T) = X_2\alpha + Y_2\beta + Z_2 = 0, \tag{7}$$

where X_1, Y_1, Z_1 and X_2, Y_2, Z_2 are the real and imaginary parts of X, Y and Z. Since α and β can be solved from Eqs. (6) and (7),

$$\alpha = \frac{Y_1Z_2 - Y_2Z_1}{\Delta} \tag{8}$$

and

$$\beta = \frac{Z_1X_2 - Z_2X_1}{\Delta}, \tag{9}$$

where $\Delta = X_1Y_2 - X_2Y_1$.

The stability boundary can be preliminarily determined in the α vs. β plane for various values of ω by letting $K = 0\,\text{dB}$, $\theta = 0^\circ$ and setting $\gamma,\ldots,T$, to constant values. Furthermore, the locus in the α vs. β plane is a boundary of the constant gain margin if K is assumed to be equal to another constant and $\theta = 0^\circ$. However, the locus is a boundary of the constant phase margin if $K = 0\,\text{dB}$ and θ is assumed to be equal to another constant. Additionally, when the third parameter γ is considered, the three aforementioned boundaries can also be found in parameter space for each specific value of γ [10].

2.2. Gain–phase margin analysis

In [9], the limit-cycle features of the nonlinear control system were analyzed by plotting the M-locus of the describing functions in the parameter plane. According to the extended definitions of M-locus [13,14], the M-locus called M_{GM} is associated to the gain margin for asymptotic stability and depends on A, ω and K. However, the M-locus called M_{PM} is related to the phase margin for asymptotic stability and depends on A, ω and θ. Notably, M_{GM} equals M_{PM} when the describing functions of the nonlinearities depend on the amplitude and not on the frequency, but not when they depend on both amplitude and frequency.

This study presents a simple method for determining the GM and PM and for plotting the loci of M_{GM} and M_{PM} in the parameter plane. Let $\theta = 0^\circ$ and adapt Eq. (4) as follows:

$$f(\alpha,\beta,\gamma,\ldots,K,j\omega T) = EK + F = 0. \tag{10}$$

Dividing Eq. (10) into real and imaginary parts yield,

$$f_R(\alpha,\beta,\gamma,\ldots,K,\omega T) = E_1K + F_1 = 0 \tag{11}$$

and

$$f_I(\alpha,\beta,\gamma,\ldots,K,\omega T) = E_2K + F_2 = 0, \tag{12}$$

where E_1, E_2, F_1 and F_2 are functions of $\alpha, \beta, \gamma, \ldots$ and ωT. Thus, K can be determined from Eqs. (11) and (12), yielding

$$K = \frac{-F_1}{E_1} \triangleq K' \tag{13}$$

and

$$K = \frac{-F_2}{E_2} \triangleq K''. \tag{14}$$

If $K' = K'' = K_i$ for $A = A_i$, then A_i and K_i, related to ω_i, can be found by varying A from 0 to ∞. For many values of ω, a set (GM) of desired values of A and K can be obtained and connected to form the M_{GM} locus in the parameter plane. Let $K = 0\,\mathrm{dB}$, and again adapt Eq. (4) as follows:

$$f(\alpha, \beta, \gamma, \ldots, \theta, \mathrm{j}\omega T) = U \cos\theta + V \sin\theta + W = 0. \tag{15}$$

Also dividing Eq. (15) into real and imaginary parts yield,

$$f_{\mathrm{R}}(\alpha, \beta, \gamma, \ldots, \theta, \omega T) = U_1 \cos\theta + V_1 \sin\theta + W_1 = 0 \tag{16}$$

and

$$f_{\mathrm{I}}(\alpha, \beta, \gamma, \ldots, \theta, \omega T) = U_2 \cos\theta + V_2 \sin\theta + W_2 = 0, \tag{17}$$

where U_1, V_1, W_1, U_2, V_2 and W_2 are functions of $\alpha, \beta, \gamma, \ldots$, and ωT. Therefore, θ can be determined from Eqs. (16) and (17), which yield

$$\theta = \cos^{-1}\left(\frac{V_1 W_2 - V_2 W_1}{U_1 V_2 - U_2 V_1}\right) \triangleq \theta' \tag{18}$$

and

$$\theta = \sin^{-1}\left(\frac{U_1 W_2 - U_2 W_1}{U_1 V_2 - U_2 V_1}\right) \triangleq \theta''. \tag{19}$$

If $\theta' = \theta'' = \theta_i$ for $A = A_i$, then A_i and θ_i, related to ω_i, can be determined by varying A from 0 to ∞. For many values of ω, a set (PM) of desired values of A and θ can be obtained and connected to form the M_{PM} locus in the parameter plane.

Based on the above analysis, after the boundaries of constant gain and phase margins have been plotted, the gain and phase margins at the corresponding intersections of these boundaries and the M_{GM} and M_{PM} loci can be determined. Moreover, the GM and the PM can both be plotted against A. If any two adjustable parameters in the asymptotically stable region are considered to analyze the stability margin, then $\mathrm{GM}_{\mathrm{min}}$ and $\mathrm{PM}_{\mathrm{min}}$ defined as the minimum values of GM and PM are the minimum amounts by which the loop gain and phase shift should be increased to produce a limit cycle solution.

3. One nonlinearity analysis

A block diagram of an aircraft pitch sampled-data control system with one nonlinear element is shown in Fig. 2. The following numerical data are used [17].

$$G_1(z) = \frac{K_c z}{(z - z_c)}, \tag{20}$$

$$G_2(s) = \frac{1}{s + 10}, \tag{21}$$

$$G_3(s) = \frac{1}{s}, \tag{22}$$

$$G_4(s) = \frac{3(s + 0.4)}{s^2 + 0.9s + 8}. \tag{23}$$

The transfer function of the zero-order hold (ZOH) is given as

$$G_{ho}(s) = \frac{1 - e^{-Ts}}{s}, \tag{24}$$

where the sampling period $T = 0.1$ s.

The nonlinearity N represents the relay with hysteresis. Assume that the input signal to N is $x(t) = A \sin \omega t$ and the describing function is as follows [18]

$$\begin{aligned} N(A) &= N_R(A) + jN_I(A) \\ &= \frac{2M}{\pi A}\left(\left(1 - \frac{d^2}{A^2}\right)^{1/2} - \left(1 - \frac{p^2}{A^2}\right)^{1/2}\right) + j\left(-\frac{2M(p-d)}{\pi A^2}\right), \quad A > p, \end{aligned} \tag{25}$$

where $M = 1$, $p = 0.1$ and $d = 1$.

Remark 3.1. N observably depends on amplitude rather than on frequency, so only one M-locus needs to be considered ($M_{GM} = M_{PM}$).

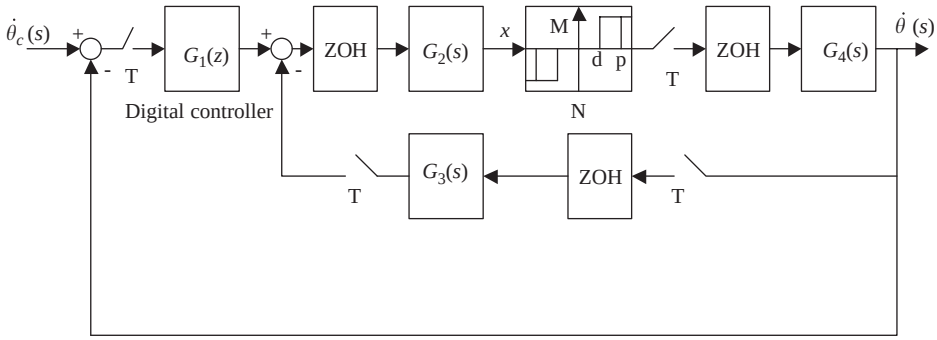

Fig. 2. Block diagram of an aircraft pitch sampled-data control system.

The overall open-loop transfer function is

$$G(z) = \frac{G_1(z)Z_{\mathrm{tf}}[G_{\mathrm{ho}}(s)G_2(s)]N(A)Z_{\mathrm{tf}}[G_{\mathrm{ho}}(s)G_4(s)]}{1 + Z_{\mathrm{tf}}[G_{\mathrm{ho}}(s)G_2(s)]N(A)Z_{\mathrm{tf}}[G_{\mathrm{ho}}(s)G_3(s)]Z_{\mathrm{tf}}[G_{\mathrm{ho}}(s)G_4(s)]}$$
$$= \frac{K_{\mathrm{c}}N(A)z(0.0183z^2 - 0.0358z + 0.0175)}{(z - z_{\mathrm{c}})(z^4 - 3.21z^3 + 3.795z^2 - 1.926z + 0.336 + N(A)(0.0018z - 0.00175))}, \tag{26}$$

where $Z_{\mathrm{tf}}[\bullet]$ denotes "the z-transform of $[\bullet]$." When the gain–phase margin tester is cascaded to the open-loop system, the characteristic equation becomes

$$\begin{aligned} f(z) &= (z - z_{\mathrm{c}})(z^4 - 3.21z^3 + 3.795z^2 - 1.926z + 0.336 \\ &\quad + N(A)(0.0018z - 0.00175)) \\ &\quad + K\mathrm{e}^{-\mathrm{j}\theta}K_{\mathrm{c}}N(A)z(0.0183z^2 - 0.0358z + 0.0175) \\ &= K\mathrm{e}^{-\mathrm{j}\theta}N(A)z(0.0183z^2 - 0.0358z + 0.0175)K_{\mathrm{c}} + (-1)(z^4 - 3.21z^3 \\ &\quad + 3.795z^2 - 1.926z + 0.336 + N(A)(0.0018z - 0.00175))z_{\mathrm{c}} \\ &\quad + z(z^4 - 3.21z^3 + 3.795z^2 - 1.926z + 0.336 + N(A)(0.0018z - 0.00175)) \\ &= X\alpha + Y\beta + Z = 0, \end{aligned} \tag{27}$$

where $\alpha = K_{\mathrm{c}}$ and $\beta = z_{\mathrm{c}}$ are adjustable parameters,

$$X = K\mathrm{e}^{-\mathrm{j}\theta}N(A)z(0.0183z^2 - 0.0358z + 0.0175), \tag{28}$$

$$Y = -(z^4 - 3.21z^3 + 3.795z^2 - 1.926z + 0.336 + N(A)(0.0018z - 0.00175)) \tag{29}$$

and

$$Z = z(z^4 - 3.21z^3 + 3.795z^2 - 1.926z + 0.336 + N(A)(0.0018z - 0.00175)). \tag{30}$$

Substituting $z = \mathrm{e}^{\mathrm{j}\omega T}$ into Eq. (27), enables α and β to be plotted according to the boundaries with fixed amplitude A (with ω varied from 0 to ∞) and fixed frequency ω (with A varied from 0 to ∞) in the K_{c} vs. z_{c} plane, as shown in Fig. 3. These boundaries distinguish two regions, one of which is the asymptotically stable region and the other of which is the limit-cycle region. Two curves ($A = 1$ and $\omega = 7$) pass through Q_1 (limit cycle region: $K_{\mathrm{c}} = 14.5$, $z_{\mathrm{c}} = 0.32$), and one limit cycle can be determined. If another point, Q_2 (asymptotically stable region: $K_{\mathrm{c}} = 2$, $z_{\mathrm{c}} = -0.4$), is also selected, then the time simulation of these two points is shown in Fig. 4, which is consistent with Fig. 3.

Secondly, two parameters $\alpha = N_{\mathrm{R}}(A)$ and $\beta = N_{\mathrm{I}}(A)$ are selected. Then, the stability boundary ($K = 0\,\mathrm{dB}$, $\theta = 0^\circ$) of Q_2 can be determined in the N_{R} vs. N_{I} plane and is represented as a thick solid line in Fig. 5. The stability boundary does not intersect the M-locus in the parameter plane, so no limit cycle is formed. When the gain or phase is increased, an intersection may arise and the limit cycle will then

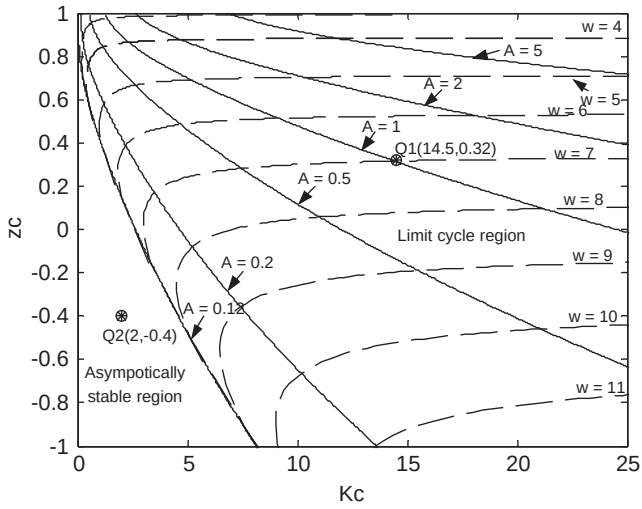

Fig. 3. Limit cycle loci in the parameter plane.

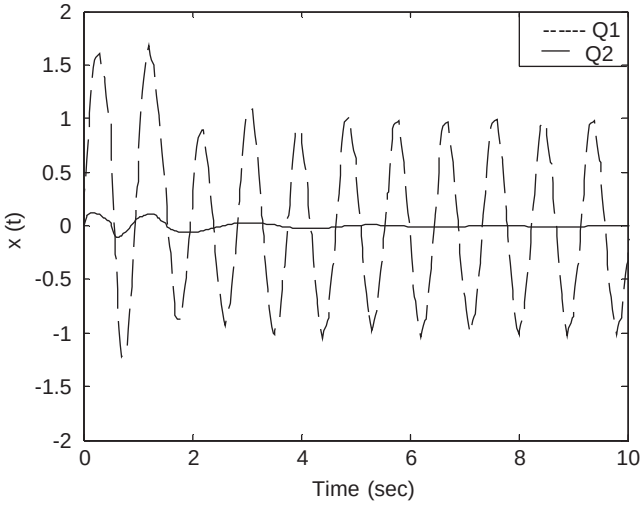

Fig. 4. Time simulation of two points in the parameter plane.

be produced. Finally, the relationship between the gain–phase margin and the characteristics of the limit cycles can be determined by the following analysis.

Let $\theta = 0^\circ$; Eq. (27) is rearranged as follows:

$$\begin{aligned} f(z) &= K_c N(A) z(0.0183z^2 - 0.0358z + 0.0175)K + (z - z_c)(z^4 - 3.21z^3 + 3.795z^2 \\ &\quad - 1.926z + 0.336 + N(A)(0.0018z - 0.00175)), \\ &= EK + F = 0, \end{aligned} \tag{31}$$

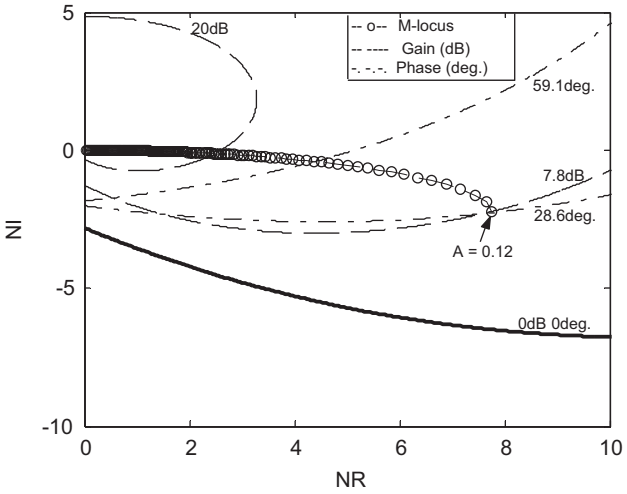

Fig. 5. *M*-locus and boundaries of constant gain–phase margin in the parameter plane.

where

$$E = K_c N(A) z(0.0183z^2 - 0.0358z + 0.0175) \tag{32}$$

and

$$F = (z - z_c)(z^4 - 3.21z^3 + 3.795z^2 - 1.926z + 0.336 + N(A)(0.0018z - 0.00175)). \tag{33}$$

Substituting $z = e^{j\omega T}$ into Eq. (31) and varying A from 0 to ∞ yields a set of A_i and K_i, related to ω_i, can be obtained directly from Eqs. (11) to (14). Let $K = 0\,\mathrm{dB}$. Eq. (27) is rearranged as follows

$$\begin{aligned} f(z) &= K_c N(A) z(0.0183z^2 - 0.0358z + 0.0175)\cos\theta \\ &\quad + K_c N(A) z(0.0183z^2 - 0.0358z + 0.0175)(-j)\sin\theta \\ &\quad + (z - z_c)(z^4 - 3.21z^3 + 3.795z^2 - 1.926z + 0.336 \\ &\quad + N(A)(0.0018z - 0.00175)) \\ &= U\cos\theta + V\sin\theta + W = 0, \end{aligned} \tag{34}$$

where

$$U = K_c N(A) z(0.0183z^2 - 0.0358z + 0.0175), \tag{35}$$

$$V = K_c N(A) z(0.0183z^2 - 0.0358z + 0.0175)(-j) \tag{36}$$

and

$$W = (z - z_c)(z^4 - 3.21z^3 + 3.795z^2 - 1.926z + 0.336 + N(A)(0.0018z - 0.00175)). \tag{37}$$

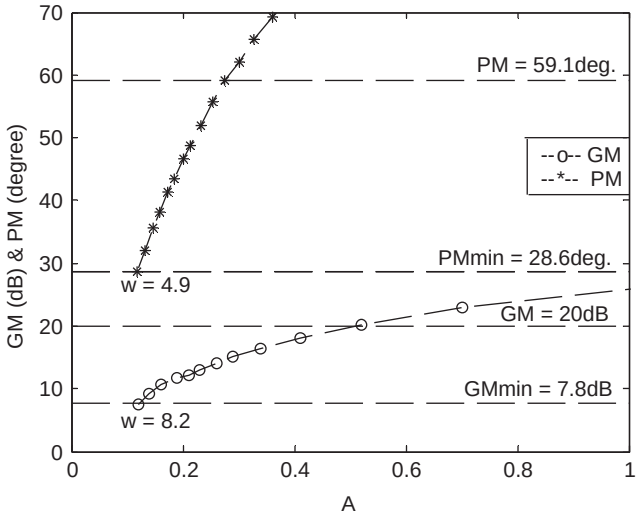

Fig. 6. The intersection points between M-locus and boundaries of constant gain–phase margin.

Substituting $z = e^{j\omega T}$ into Eq. (34) and varying A from 0 to ∞ enables a set of A_i and θ_i, related to ω_i, to be directly obtained from Eqs. (16)–(19).

Based on the analysis in the above paragraph, if Q_2 ($K_c = 2,\ z_c = -0.4$) is to be analyzed, then the margins of gain and phase associated with the limit cycle are obtained from Fig. 6. Therefore, two curves ($GM_{min} = 7.8\,dB$ and $PM_{min} = 28.6^\circ$) are tangent to the M-locus and produce the limit cycle. The amplitude and the frequency of the limit cycles due to other values of GM (K) and PM (θ) can be directly obtained from Fig. 6. The time responses of the limit cycle obtained by substituting $K = 7.8$ and 20 dB are shown in Fig. 7. However, the time responses of the limit cycle obtained by substituting $\theta = 28.6^\circ$ and 59.1° are shown in Fig. 8. The simulation results in Figs. 7 and 8 are consistent with Fig. 6.

4. Analyzing multiple nonlinearities

This section will address the limit cycle analysis of a nonlinear sampled-data system with multiple nonlinearities. The related block diagram is displayed in Fig. 9. The following numerical data are used [14].

$$G_1(z) = \frac{K_c z}{(z - z_c)}, \tag{38}$$

$$G_2(s) = \frac{1}{(10s + 1)^2}, \tag{39}$$

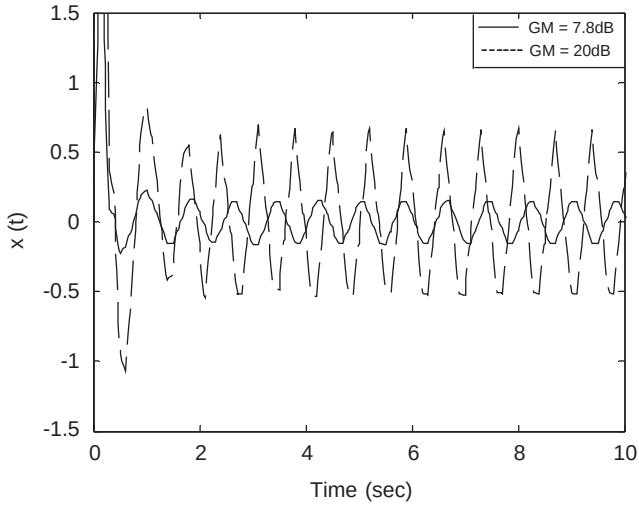

Fig. 7. Simulation results of limit cycle with increased gain.

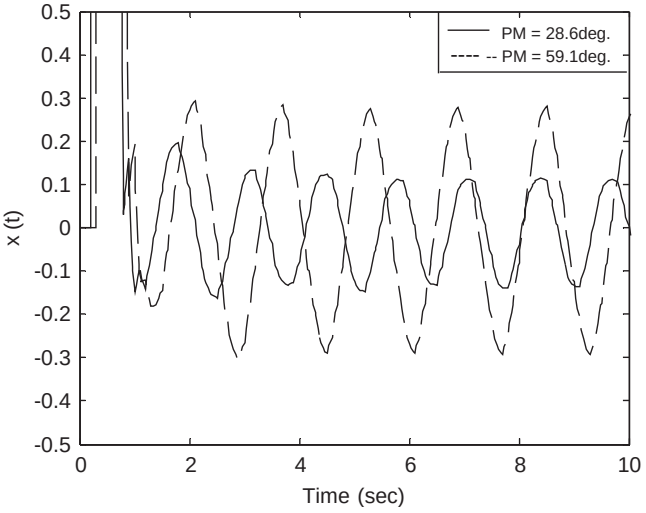

Fig. 8. Simulation results of limit cycle with increased phase.

$$G_3(s) = \frac{1}{s}, \tag{40}$$

$$G_4(s) = \frac{10s}{0.5s + 1}, \tag{41}$$

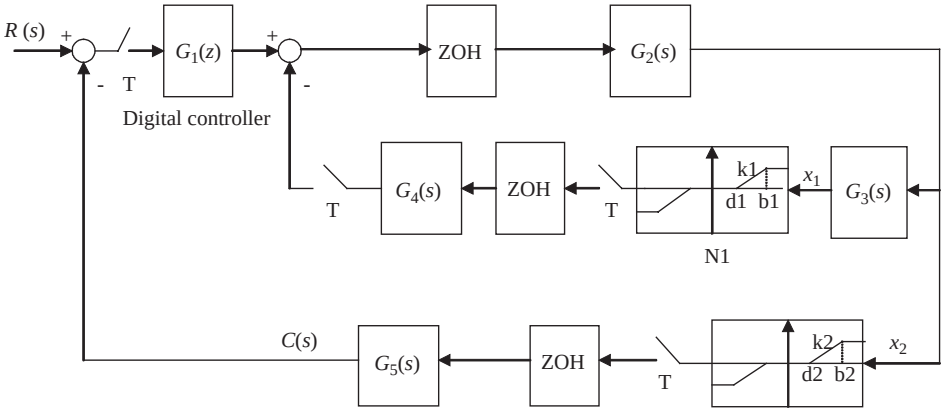

Fig. 9. Block diagram of a sampled-data control system with multiple nonlinearities.

$$G_5(s) = \frac{1}{2s^2 + s}. \tag{42}$$

where the sampling period is $T = 1$ s.

The nonlinearities N_1 and N_2 represent the saturation with a dead zone. Assume that the input signals to N_1 and N_2 are $x_1(t) = A_1 \cos \omega t$ and $x_2(t) = A_2 \sin \omega t$, respectively, and the describing functions are as follows [18]

$$N_m(A_m) = \frac{2k_m}{\pi}\left(\sin^{-1}\left(\frac{b_m}{A_m}\right) - \sin^{-1}\left(\frac{d_m}{A_m}\right) + \frac{b_m}{A_m}\left(1 - \frac{b_m^2}{A_m^2}\right)^{1/2} - \frac{d_m}{A_m}\left(1 - \frac{d_m^2}{A_m^2}\right)^{1/2}\right), \quad A_m > b_m,\ m = 1, 2, \tag{43}$$

where $k_1 = 1$, $b_1 = 3$, $d_1 = 1$, $k_2 = 1$, $b_2 = 2$ and $d_2 = 1$.

Remark 4.1. If $x_2(t)$ is adopted as the reference input signal for analysis, then A_1 can be expressed as a function of A_2 and ω, $A_1 = A_2/\omega$, so N_1 depends on the amplitude and the frequency when A_2 and ω are specified, revealing that M_{GM} and M_{PM} must be considered, respectively.

The overall open-loop transfer function is

$$\begin{aligned} G(z) &= \frac{G_1(z)Z_{tf}[G_{ho}(s)G_2(s)]N_2(A_2)Z_{tf}[G_{ho}(s)G_5(s)]}{1 + Z_{tf}[G_{ho}(s)G_2(s)G_3(s)]N_1(A_1)Z_{tf}[G_{ho}(s)G_4(s)]} \\ &= \frac{0.001K_cN_2(A_2)z(z^6 - 1.16z^5 - 1.44z^4 + 1.85z^3 + 0.4z^2 - 0.73z + 0.087)}{(z - z_c)(z^9 - 6.36z^8 + 17.4z^7 - 26.62z^6 + 24.76z^5 - 14.19z^4 + 4.8z^3 - 0.85z^2} \\ &\quad + 0.055 + N_1(A_1)(0.032z^8 - 0.019z^7 - 0.26z^6 + 0.59z^5 - 0.5z^4 + 0.14z^3 \\ &\quad + 0.02z^2 - 0.014)). \end{aligned} \tag{44}$$

When the gain–phase margin tester is cascaded to the open-loop system, the characteristic equation becomes

$$\begin{aligned} f(z) &= (z - z_c)(z^9 - 6.36z^8 + 17.4z^7 - 26.62z^6 + 24.76z^5 - 14.19z^4 + 4.8z^3 \\ &\quad - 0.85z^2 + 0.055 + N_1(A_1)(0.032z^8 - 0.019z^7 - 0.26z^6 + 0.59z^5 \\ &\quad - 0.5z^4 + 0.14z^3 + 0.02z^2 - 0.014)) + Ke^{-j\theta}0.001K_cN_2(A_2)z(z^6 - 1.16z^5 \\ &\quad - 1.44z^4 + 1.85z^3 + 0.4z^2 - 0.73z + 0.087) \\ &= X\alpha + Y\beta + Z = 0. \end{aligned} \tag{45}$$

Firstly, two adjustable parameters $\alpha = K_c$ and $\beta = z_c$ are selected. Then substituting $z = e^{j\omega T}$ into Eq. (45), enables α and β to be determined from Eqs. (6)–(9). Taking $K = 0\,\text{dB}$ and $\theta = 0^\circ$ enables solutions for α and β to be plotted from the boundaries with a fixed amplitude A_2 (with ω varied from 0 to ∞) and a fixed frequency ω (with A_2 varied from 0 to ∞) in the K_c vs. z_c plane, as shown in Fig. 10. These boundaries distinguish two regions, one of which is the asymptotically stable region and the other of which is the limit-cycle region. Four curves ($A_2 = 1.5$ and 56, $\omega = 0.08$ and 0.27) pass through Q_1 (limit cycle region: $K_c = 3.7$, $z_c = 0.33$), and two limit cycles can be determined as follows:

(1) stable limit cycle ($A_2 = 56,\ \omega = 0.08$);
(2) unstable limit cycle ($A_2 = 1.5$, $\omega = 0.27$).

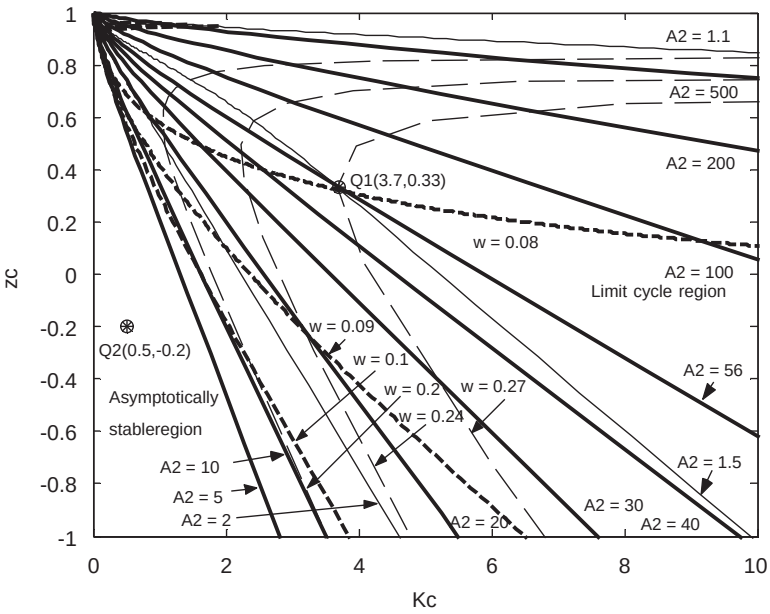

Fig. 10. Limit cycle loci in the parameter plane.

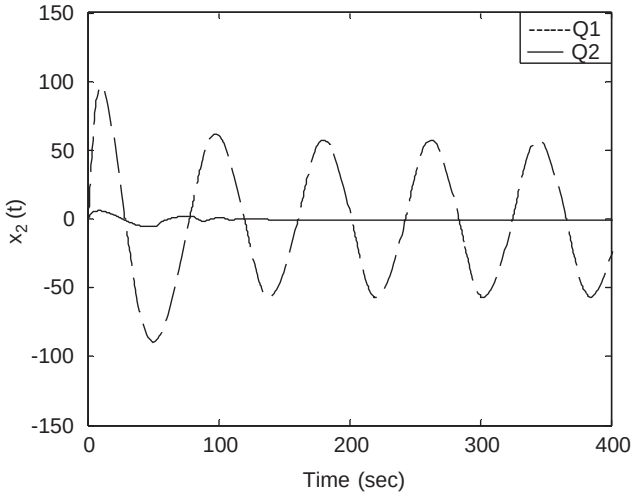

Fig. 11. Time simulation of two points in the parameter plane.

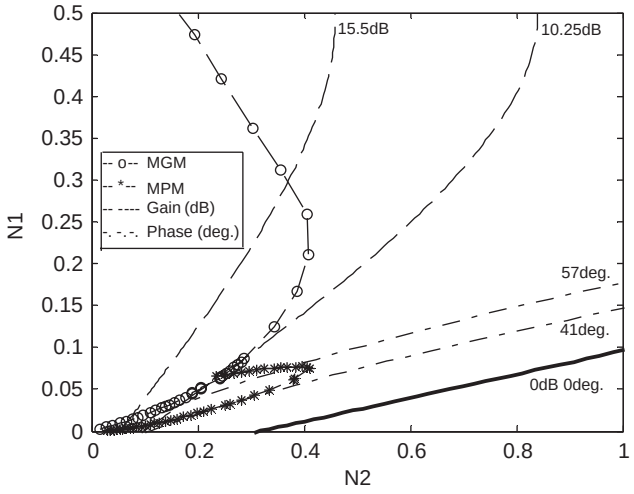

Fig. 12. *M*-loci and boundaries of constant gain–phase margin in the parameter plane.

The time simulation in Fig. 11 depicts the results associated with point Q_2 (asymptotically stable region: $K_c = 0.5$, $z_c = -0.2$) from Fig. 10.

Two parameters $\alpha = N_2(A_2)$ and $\beta = N_1(A_1)$ are similarly considered. Accordingly, the stability boundary of Q_2 can be identified in the N_2 vs. N_1 plane and is represented as a thick solid line in Fig. 12. Notably, the stability boundary does not intersect the *M*-loci (M_{GM} and M_{PM}) in the parameter plane and no limit cycle is

generated. However, if the gain or phase is increased, the limit cycles can be predicted since the intersection occurs.

Finally, the gain–phase margin analysis of the nonlinear system is considered. Rearranging Eq. (45) and letting $\theta = 0^\circ$ yield

$$\begin{aligned} f(z) &= 0.001N_2(A_2)z(z^6 - 1.16z^5 - 1.44z^4 + 1.85z^3 + 0.4z^2 - 0.73z + 0.087)K \\ &\quad + (z - z_c)(z^9 - 6.36z^8 + 17.4z^7 - 26.62z^6 + 24.76z^5 - 14.19z^4 + 4.8z^3 \\ &\quad - 0.85z^2 + 0.055 + N_1(A_1)(0.032z^8 - 0.019z^7 - 0.26z^6 + 0.59z^5 \\ &\quad - 0.5z^4 + 0.14z^3 + 0.02z^2 - 0.014)) \\ &= EK + F = 0. \end{aligned} \tag{46}$$

Substituting $z = e^{j\omega T}$ into Eq. (46) and varying A_2 from 0 to ∞ enables a set of A_{2i} and K_i, related to ω_i, to be obtained directly from Eqs. (11) to (14). Let $K = 0\,\mathrm{dB}$. Eq. (45) can be rearranged as follows:

$$\begin{aligned} f(z) &= 0.001K_cN_2(A_2)z(z^6 - 1.16z^5 - 1.44z^4 + 1.85z^3 + 0.4z^2 - 0.73z \\ &\quad + 0.087)\cos\theta + 0.001K_cN_2(A_2)z(z^6 - 1.16z^5 - 1.44z^4 + 1.85z^3 \\ &\quad + 0.4z^2 - 0.73z + 0.087)(-j)\sin\theta + (z - z_c)(z^9 - 6.36z^8 + 17.4z^7 \\ &\quad - 26.62z^6 + 24.76z^5 - 14.19z^4 + 4.8z^3 - 0.85z^2 + 0.055 + N_1(A_1) \\ &\quad \times(0.032z^8 - 0.019z^7 - 0.26z^6 + 0.59z^5 - 0.5z^4 \\ &\quad + 0.14z^3 + 0.02z^2 - 0.014)) \\ &= U\cos\theta + V\sin\theta + W = 0. \end{aligned} \tag{47}$$

Substituting $z = e^{j\omega T}$ into Eq. (47) and varying A_2 from 0 to ∞ enables a set of A_{2i} and θ_i, related to ω_i, also to be obtained directly from Eqs. (16)–(19).

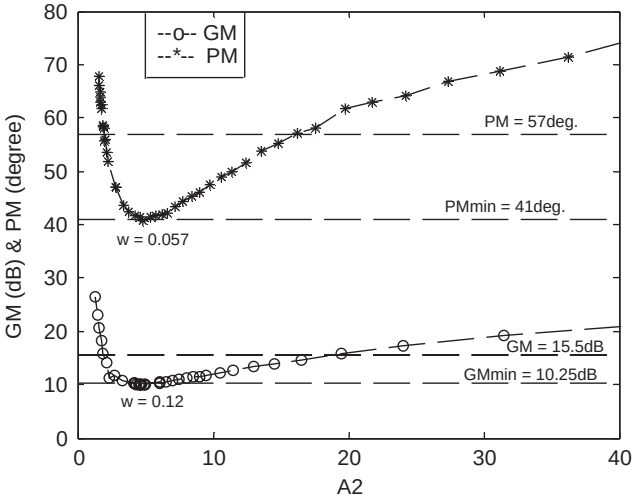

Fig. 13. The intersection points between M-loci and boundaries of constant gain–phase margin.

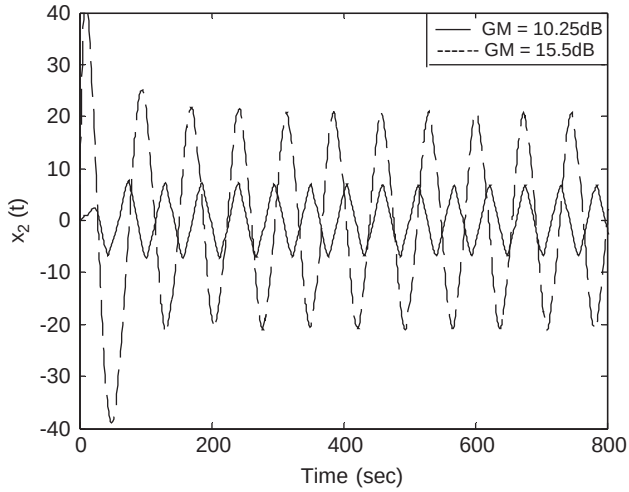

Fig. 14. Simulation results of limit cycle with increased gain.

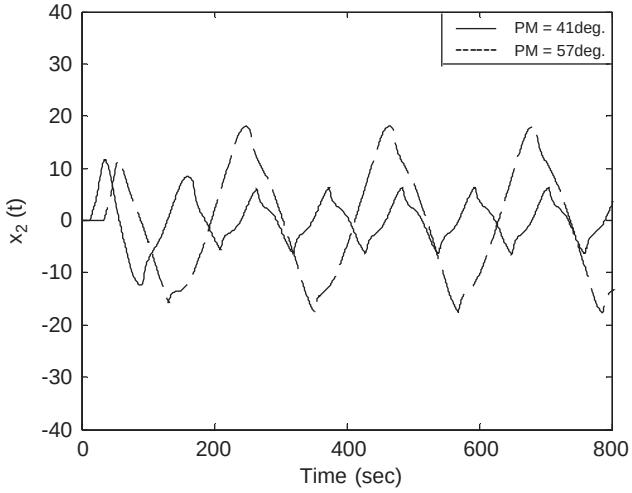

Fig. 15. Simulation results of limit cycle with increased phase.

The relationship between the gain–phase margins and the amplitude of the limit cycle of Q_2 is shown in Fig. 13. Two conditions of gain margin ($GM_{min} = 10.25\,dB$ and $GM = 15.5\,dB$) in Fig. 13 are illustrated to check the accuracy. In Fig. 14, when K is increased to 10.25 dB, a limit cycle is yielded implying that the system shifted from an asymptotically stable region to a limit cycle region. Again, increasing the gain to 15.5 dB yields two limit cycles of which one is stable and the other one is unstable. Notably, the unstable limit is not easily observed, so Fig. 14 depicts only

one stable limit cycle. Two other phase margin ($PM_{min} = 41^\circ$ and $PM = 57^\circ$) conditions are considered and the simulation results in Fig. 15 match those in Fig. 13.

5. Conclusions

Some effective methods, including gain–phase margin tester technology, the *M*-locus method and the parameter plane method, were integrated to predict the limit cycles of a nonlinear sampled-data control system. A simple method for determining the gain–phase margins and plotting the *M*-locus for limit cycle analysis is developed. The results of this study demonstrate that the gain–phase margin analysis of limit cycles of a nonlinear continuous-data system can be easily extended to a sampled-data system using the proposed approach.

Acknowledgements

The authors would like to thank Prof. K.W. Han for his guidance and suggestion. This paper was supported by the ROC Ministry of Education under Grant 91X104 EX-91-E-FA06-4-4.

References

[1] C.S. Cox, I.G. French, Limit cycle prediction conditions for hydraulic control system, ASME J. Dyn. Syst. Meas. Control 108 (1986) 17–23.
[2] H. Olsson, K.J. Astrom, Friction generated limit cycles, IEEE Trans. Control Syst. Technol. 9 (2001) 629–636.
[3] J. Ackermann, T. Bunte, Actuator rate limits in robust car steering control, Proceedings of the IEEE Conference on Decision & Control, 1997, pp. 4726–4731.
[4] F. Amato, R. Iervolino, M. Pandit, L. Verde, Analysis of pilot-in-the-loop oscillations due to position and rate saturations, Proceedings of the IEEE Conference on Decision & Control, 1999, pp. 3564–3569.
[5] K.W. Han, G.J. Thaler, Control system analysis and design using a parameter space method, IEEE Trans. Autom. Control 11 (3) (1996) 560–563.
[6] J. Ackermann, Parameter space design of robust control systems, IEEE Trans. Autom. Control 25 (6) (1980) 1058–1072.
[7] A. Cavallo, G.E. Maria, L. Verde, Robust control systems: a parameter space design, J. Guidance Control Dyn. 15 (5) (1992) 1207–1215.
[8] D.D. Siljak, Parameter space methods for robust control design: a guide tour, IEEE Trans. Autom. Control 34 (7) (1989) 674–688.
[9] D.D. Siljak, Nonlinear Systems—the Parameter Analysis and Design, Wiley, New York, 1969.
[10] C.H. Chang, K.W. Han, Gain margins and phase margins for control systems with adjustable parameters, J. Guidance Control Dyn. 13 (3) (1990) 404–408.
[11] C.H. Chang, K.W. Han, Gain margin and phase margin analysis of a nuclear reactor control system with multiple transport lags, IEEE Trans. Nucl. Sci. 36 (4) (1989) 1418–1425.
[12] C.H. Chang, K.W. Han, Gain margins and phase margins for sampled-data control systems with adjustable parameters, IEE Proc. Control Theory Appl. 138 (3) (1991) 285–291.

[13] C.H. Chang, M.K. Chang, Analysis of gain margins and phase margins of a nonlinear reactor control system, IEEE Trans. Nucl. Sci. 41 (4) (1994) 1686–1691.
[14] M.K. Chang, C.H. Chang, K.W. Han, Gain margins and phase margins for nonlinear control systems with adjustable parameters, Proceedings of the IEEE Conference on Industry and Application, 1993, pp. 2123–2130.
[15] Y.C. Chang, K.W. Han, Analysis of limit cycles for a low flying vehicle with three nonlinearities, Int. J. Actual Probl. Aviat. Aerosp. Systems USSR 6 (2) (1998) 38–50.
[16] B.F. Wu, J.W. Perng, Gain–phase margin analysis of pilot-induced oscillations for limit cycle prediction, J. Guidance Control Dyn. 27 (1) (2004) 59–65.
[17] Y.K. Cheng, K.W. Han, G.J. Thaler, Analysis of nonlinear control system with transport lag, IEEE Trans. Ind. Gen. Appl. IGA-7 (5) (1971) 576–579.
[18] K.W. Han, Nonlinear Control Systems—Some Practical Methods, Academic Cultural Company, California, 1977.